Millimeter-Wave Characteristics of Phase-Correcting Fresnel Zone Plates

DONALD N. BLACK, STUDENT MEMBER, IEEE, AND JAMES C. WILTSE, FELLOW, IEEE

Abstract—**A focusing element called the phase-correcting Fresnel zone plate is described, and its characteristics are given when used in the millimeter-wave region for imaging or frequency filtering in place of a lens. Two versions are discussed, one where alternate concentric annular grooves are cut in a single piece of low-loss dielectric, and a second where two (or more) dielectrics are used in alternate concentric rings. For the latter case, an appropriate choice of parameters produces a design of constant thickness (i.e., a flat disk), named the "planar lens." Design formulas and curves, as well as measured results, are given for both types, and an analytical description is derived for the far-field patterns. Compared with lenses, zone plates are simpler to construct and have lower absorption loss, thickness, and weight.**

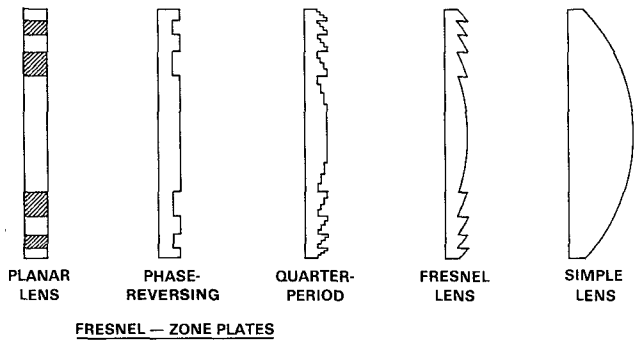

Fig. 1. Relation between zone plates and lenses.

I. Introduction

THE FRESNEL ZONE plate, a planar device which has lens-like properties, can be used for focusing and imaging electromagnetic waves [1]–[3]. Zone plates accomplish these functions through diffraction and interference, rather than refraction. This paper describes two types of phase-correcting zone plates made from low-loss dielectric material. The phase change is introduced in one case by cutting annular grooves in the dielectric, and in the other case by using two or more dielectrics having different dielectric constants. Fig. 1 shows cross-sectional views of these and related zone plates and lenses.

Since zone plates have flat surfaces, they are simpler to construct than conventional lenses and have the added advantages of reduced thickness, weight, and absorption loss. This is illustrated in Fig. 2, which shows the differences among lenses and a zone plate designed for operation at 140 GHz. The ideal hyperboloid lens has a complex contour which is difficult to machine, and both the hyperboloid and spherical lenses are much heavier and lossier than the zone plate. Normally, any of these elements would be fed from a horn antenna, whose main lobe pattern at least covers the lens or zone plate area. The horn would be located at the focal point in a geometry where the focal length (f) and the diameter (D) are comparable (a typical configuration).

In this paper the design relationships and observed characteristics for zone plates will be presented. These characteristics include focusing action, frequency filtering, and image deviation. The far-field pattern for zone plates is derived and compared with results expected at millimeter wavelengths. Second-order effects such as shadowing will be discussed.

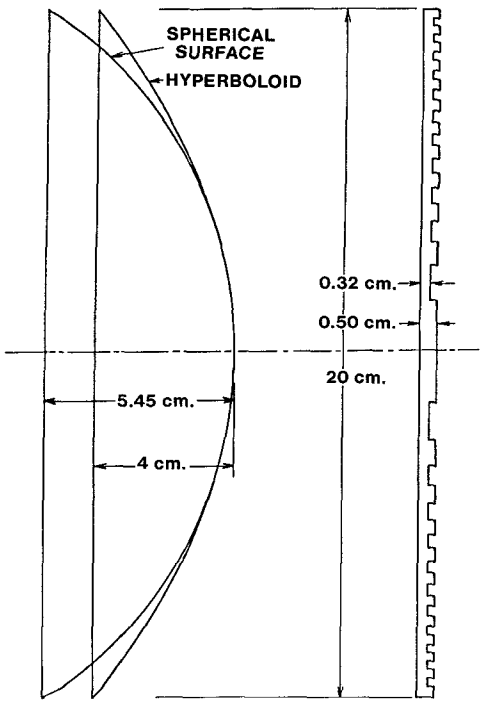

Fig. 2 Comparison of polystyrene zone plate and lenses with 20-cm focal length designed for use at 140 GHz

Manuscript received April 25, 1987; revised August 22, 1987.

The authors are with the Georgia Tech Research Institute, Georgia Institute of Technology, Atlanta, GA 30332.

IEEE Log Number 8717495.

0018-9480/87/1200-1122$01.00 ©1987 IEEE

II. Design Relations

The single-dielectric phase-correcting zone plate consists of a set of planar concentric annular rings cut into a flat piece of low-loss dielectric material, such as polystyrene. For a phase-*reversing* zone plate, the successive radii of these zones are chosen so that the distance from a selected ("focal") point on the central axis increases by *one-half* wavelength (Δ) in going from the inner to the outer radius of any ring, as illustrated in Fig. 3. If a plane wave is normally incident on the zone plate (from the left in Fig. 2), the portions of the radiation which pass through various parts of the transparent zones all reach the selected focal point with phases which differ by less than one-half period. Thus, the zone plate acts like a lens, producing a focusing action on the radiation it transmits. Using the right triangle relationship in Fig. 3, the radius of each zone, r_n, is given by

$$r_n = \sqrt{nf\lambda + (n\lambda/2)^2}.$$

A more general formula,

$$r_n = \sqrt{nf\lambda + (n\lambda/P)^2}$$

gives r_n for a zone plate which uses P different phases to implement the phase correction. For the phase-reversing zone plate, P equals 2, and for the quarter-period zone plate, P equals 4. The intensity at the focus is increased by using larger P. However, the relative increase diminishes noticeably as a P greater than 4 is used.

It should be noted that the "focal" point mentioned here is the principal or first-order focus and that higher order foci arise from the superposition of the higher diffraction orders produced by the zone plate. If the principal focus is at f, the higher order foci occur at $f/3$, $f/5$, $f/7$, etc. The usual lens relationships hold for each focus. Most of the intensity will be distributed to the principal focus [4].

The different phases for each zone are implemented by cutting annular grooves into the dielectric. For the phase-reversing zone plate, grooves of a depth d are cut into alternating zones. This d is given by $d = \lambda_0/2(\sqrt{\epsilon - 1})$ where λ_0 is the free-space wavelength and ϵ is the dielectric constant of the material. For a quarter-period zone plate, successive groove depths d', $2d'$, and $3d'$ are used in repetitive order. This depth is given by $d' = \lambda_0/4(\sqrt{\epsilon - 1})$.

Zone plates of this grooved type were first developed for millimeter waves by Sobel [1] and have been employed in a number of system applications as a replacement for lenses [5]–[7]. When properly fed by a horn antenna, the antenna pattern is similar to that obtained with a horn–lens combination, namely a narrow main lobe and major sidelobes at the angles and levels predicted from normal aperture theory. Measured patterns have been given in the literature [1], [5].

With the grooved single dielectric lens, edge scattering and shadowing from the annular grooves can occur. Measurements at 140 GHz on the zone plate shown in Fig. 2 showed numerous very low level sidelobes in both the

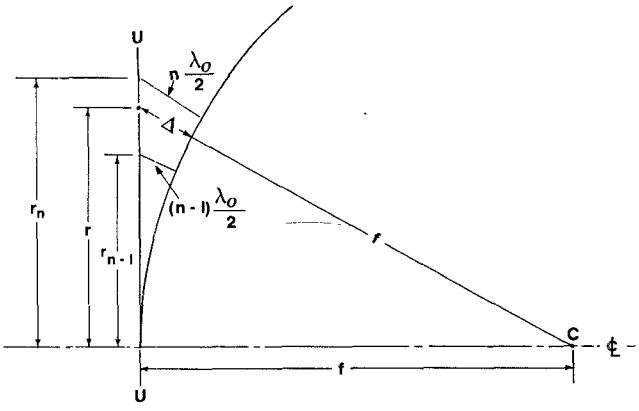

Fig. 3. Geometry of the nth zone.

E-plane and H-plane far-field patterns. For example, in the H plane a total of about 45 lobes was found, each of which was at least 30 dB below the main lobe. Of these, 35 were within $\pm 45°$ of the forward direction, and 10 within $\pm 20°$ of the backward direction. These effects may be reduced by using the planar lens (alternate annular rings of different dielectric constant, but equal thickness) to introduce the desired phase correction. This configuration has the geometrical advantage that the front and back surfaces are flat. Since the edges arising from annular grooves are absent, there is no shadowing and less scattering. In addition, the flat lens surface results in no accumulation of material on the lens and provides an aerodynamically smooth surface for easier use in airstreams.

III. Zone Plate Characteristics

The focusing effect of a half-period plate is denoted by $R(N)$, the ratio of intensity at the focus of a zone plate to the intensity at the focus without a zone plate. Here, N is the number of half-period zones and it is assumed that a uniform plane wave is normally incident on the zone plate. $R(N)$ is given by

$$R(N) = 4\left(\sum_{n-1}^{N} \frac{\frac{8f}{\lambda_0} + (2n-1)}{\frac{8f}{\lambda_0} + 2(2n-1)} \right)^2$$

where f is the focal length. For large values of f/λ_0 relative to N, the bracketed term is approximately equal to one, and $R(N) \sim 4N^2$ applies.

When the frequency ω is not the design frequency ω_0, the intensity $R(N)$ is a rather complicated function of N and of ω/ω_0. For any frequency ω,

$$\begin{aligned} R(N) = &\left(\sum_{n-1}^{N} A(n) \left\{ \cos \pi(\omega/\omega_0) \left[2\,\mathrm{GIV}\left(\frac{n-1}{2} \right) + 1 \right] \right.\right. \\ &\left.\left. - \cos \pi(\omega/\omega_0) \left[2\,\mathrm{GIV}\left(\frac{n-1}{2} \right) \right] \right\} \right)^2 \\ &+ \left(\sum_{n-1}^{N} A(n) \left\{ \sin \pi(\omega/\omega_0) \left[2\,\mathrm{GIV}\left(\frac{n-1}{2} \right) + 1 \right] \right.\right. \\ &\left.\left. - \sin \pi(\omega/\omega_0) \left[2\,\mathrm{GIV}\left(\frac{n-1}{2} \right) \right] \right\} \right)^2. \end{aligned}$$

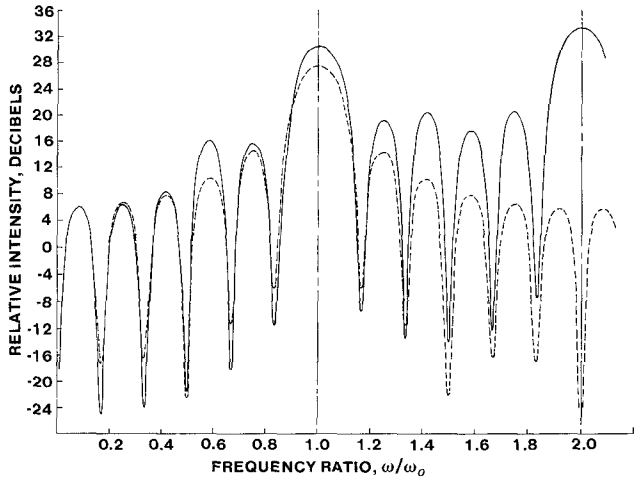

Fig. 4 Frequency characteristics of zone plate with $F = 50\lambda$. Quarter-period lens of 48 zones (solid curve); half-period lens of 24 zones.

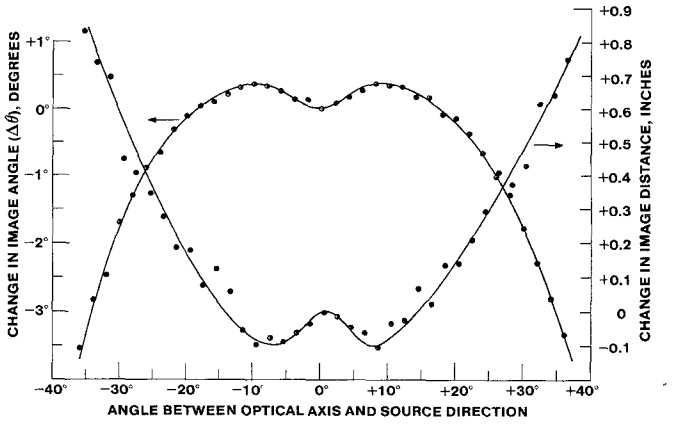

Fig. 5 Image angle displacement, 140-GHz half-period zone plate.

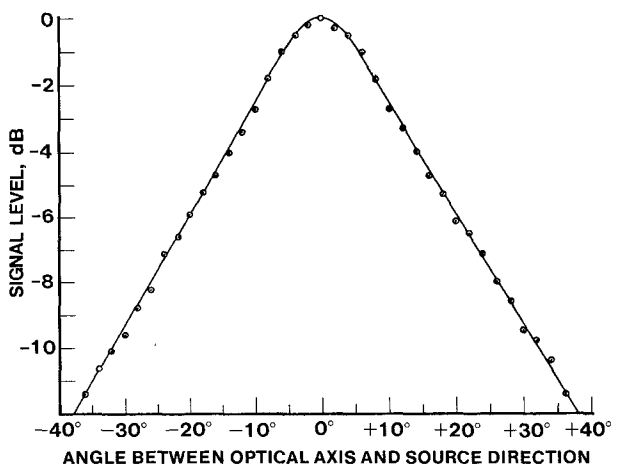

Fig. 6. Off-axis image intensity, 140-GHz half-period zone plate.

The term, $\mathrm{GIV}\left(\frac{n-1}{2}\right)$ represents the integral value of $\frac{n-1}{2}$, that is, the largest integer that is less than or just equal to $\frac{n-1}{2}$. Thus, for $n=1$ and $n=2$, $\mathrm{GIV}\left(\frac{n-1}{2}\right)=0$, and so fourth. The coefficients $A(n)$ are given by

$$A(n)=\frac{\frac{8f}{\lambda_0}+(2n-1)}{\frac{8f}{\lambda_0}+2(2n-1)}.$$

Similar relationships have been derived for the quarter-period zone plate [1]. As the number of zones is increased, the curve of $R(N)$ versus frequency ratio displays an increasing number of maxima and minima. A typical calculated frequency characteristic is shown in Fig. 4 for a zone plate having a focal length of 50 wavelengths at ω_0 and 24 half-period zones or 48 quarter-period zones. The minima in the frequency characteristic of Fig. 4 suggest employing the zone plate as a frequency filter, and this has been done in the past. For the zone plates in Fig. 4, the 3-dB bandwidth (centered at ω_0) is approximately 15 percent of ω_0. In general, for a half-period zone plate the 3-dB bandwidth in radians can be approximated by $2\omega_0/N$. This approximation is more accurate for large N. Note that a quarter-period plate designed for the frequency ω_0 acts as a half-period plate at the second harmonic.

It can be shown that the distance to the focal point is frequency dependent (analogous to chromatic aberration). Obviously, it can be arranged so that widely different frequencies focus at different points, thus producing focal isolation (a quasi-optical technique for separating different frequencies). The radiation patterns of a Fresnel zone plate fed by a horn antenna at its focal point are in good agreement with the predictions of elementary diffraction theory, and this has been confirmed by measurement. A plate with many zones generally will have many small side lobes symmetrically distributed. If no attempt is made to reduce reflections from the dielectric surfaces of the zone plate, a back lobe is present. Reflection losses for a dielectric constant of 2.5 would amount to about 0.5 dB for the case where (as an example) the amplitude reflections from the front and back surfaces of the plate are in quadrature. Nearly exact cancellation of the two reflections can be accomplished by a correct choice of thickness and dielectric constant.

One of the questions that arise in considering the application of zone plates instead of lenses is their relative off-axis image formation performance. Figs. 6–8 illustrate data from earlier unpublished work in which measurements were made at 140 GHz utilizing a 20-cm-diameter, 24-zone, half-period plate with focal length equal to the diameter (Fig. 2). One of the quantities measured was the angular deviation, or error $\Delta\theta$, between the normal to the zone plate and the source direction. The angular deviation did not exceed $\pm 0.4°$ for θ within the range of $\pm 22°$. Fig. 5 illustrates this.

A second quantity measured was the change in distance behind the center of the zone plate at which the image is found. Fig. 5 shows that if θ remains within $\pm 20°$, the change in image distance remains less than ± 0.15 in, or less than 2 percent of the focal length. A third quantity measured was the change in maximum signal level as a function of angle θ. The intensity falls off steadily but not very rapidly as the image moves away from the optical axis. From Fig. 6 it is seen that if the source direction is within $\pm 11°$ of the normal to the zone plate, the signal

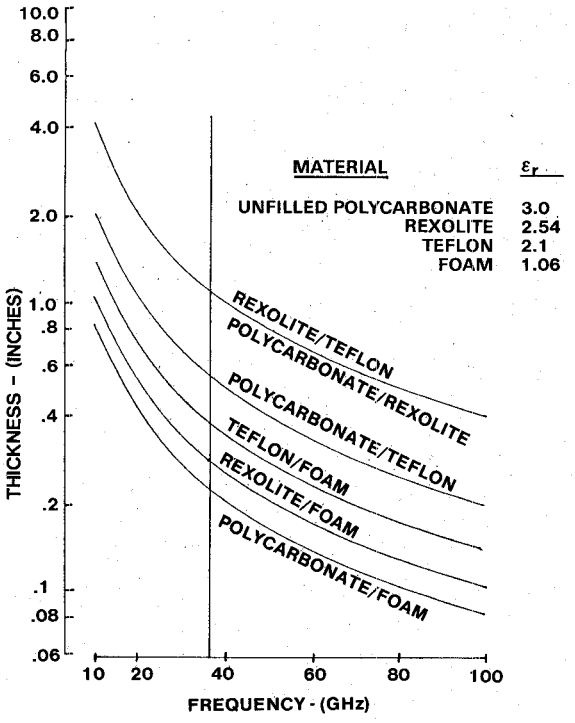

Fig. 7. Planar lens, thickness versus frequency versus materials.

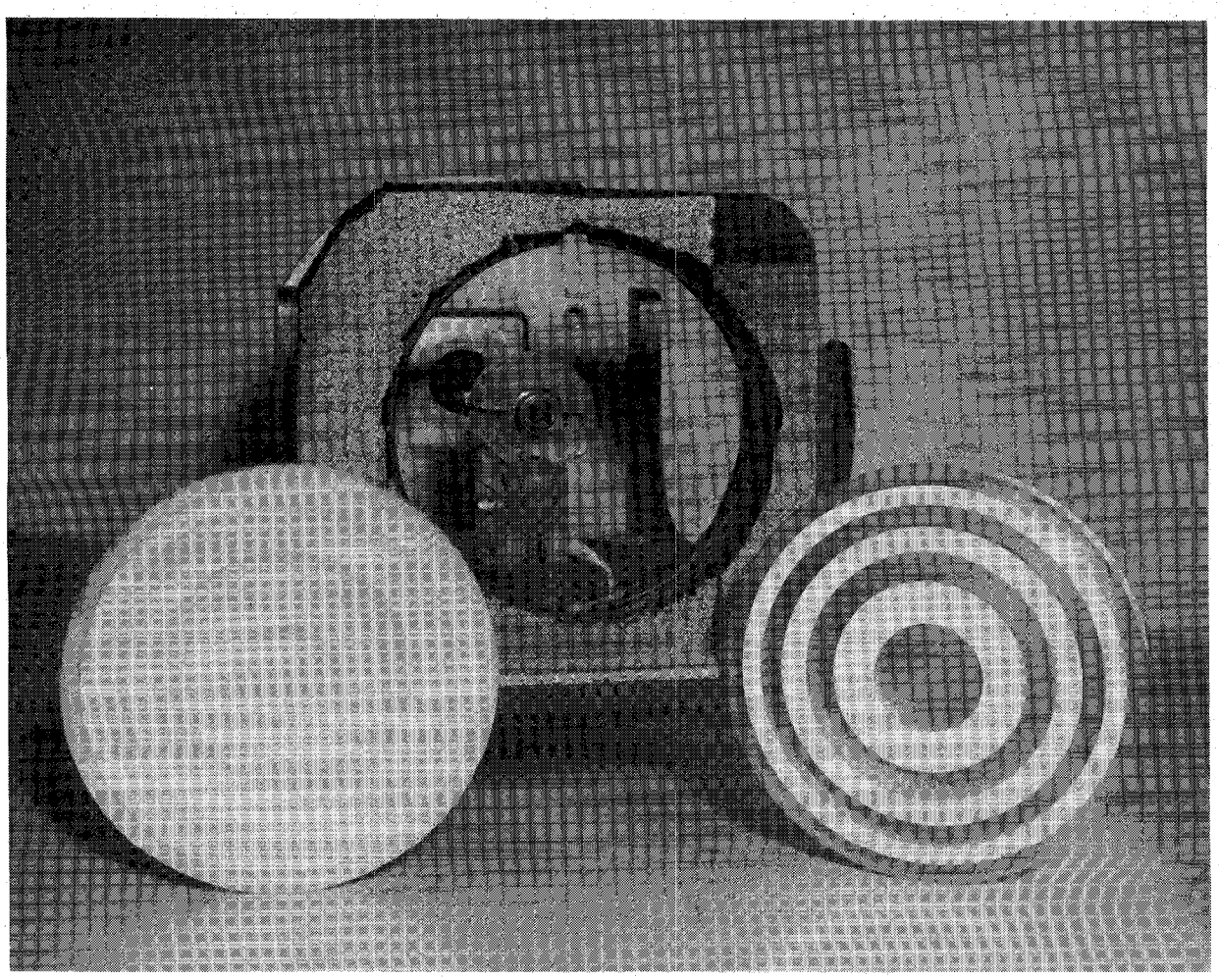

Fig. 8. Photograph of 35-GHz planar lenses (Rexolite & foam or Teflon).

decreases by less than 3 dB, and that for angles within $\pm 20°$, the signal decrease is within 6 dB.

IV. Planar Lens

The planar lens, mentioned earlier, is a different version of the phase-reversing zone plate that is constructed by using two different materials instead of alternating grooved zones. By proper choice of the two dielectrics, the zones are made equal in thickness. This was proposed by one of the present authors (Wiltse) in 1976 and was demonstrated experimentally [2].

Fig. 7 provides a graph for selecting lens thickness and dielectrics for a planar lens. The intersection of the vertical line at 35 GHz and of the material curves gives the thickness of that particular material combination required to construct a planar lens for use at 35 GHz. For example, a 35-GHz planar lens constructed from a Rexolite/foam combination would be 0.28 in thick, and one made from Teflon/foam would need to be 0.39 in thick. Fig. 8 shows a picture of a Rexolite/foam and a Rexolite/Teflon seven-zone planar lens for use at 35 GHz. The planar lens zone radii are given by the same r_n used to design single-dielectric lenses. A measured far-field pattern for the Rexolite/Teflon lens shown in Fig. 8 is plotted in Fig. 9.

V. Far-Field Pattern

The phase-corrected plate consists of a series of phased annuli together with one central aperture. To arrive at the far-field pattern for the zone plate, the far-field patterns for the individual annuli are superimposed. The first step is to derive a field expression for each annulus. Then the resulting annulus expressions are summed to obtain the far-field pattern for the lens. The basic geometry used in the derivation is shown in Fig. 10. The ρ and ϕ plane on the left contains the zone plate, and the q and Φ plane on the right is the far-field plane.

The expression for the electric field is obtained from the Kirchhoff diffraction integral (see [8, p. 9-7]). Using the far-field simplifications as outlined in Sherman [8], the resulting electric field expression is given by

$$E(Y,Z) = (1+\cos\theta) \cdot \iint_{\text{Aperture}} \frac{e^{j[\omega t - KR]}}{R} e^{-j\delta n} F(y,z) e^{j\frac{k}{R}(Yy+Zz)} dS$$

where $e^{-j\delta n}$ is the phase factor for the aperture and $F(y,z)$ is the aperture illumination function. Converting to cylindrical coordinates and letting F be a function of ρ only [9]:

$$E(\theta) = \frac{(1+\cos\theta)e^{j(\omega t - KR)}}{R} e^{-j\delta n} \cdot \int_{r_{n-1}}^{r_n} F(\rho)\rho \int_0^{2\pi} e^{jK\rho\sin\theta\cos\phi}\, d\rho d\phi$$

where r_{n-1} is the inner radius of the aperture and r_n is the outer radius. Note that

$$r_n > r_{n-1} > 0.$$

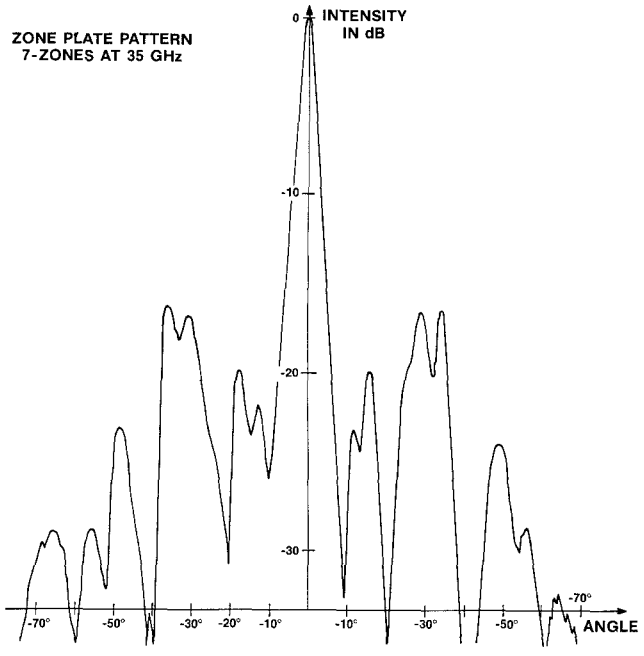

Fig. 9 Far-field pattern for 35-GHz planar lens.

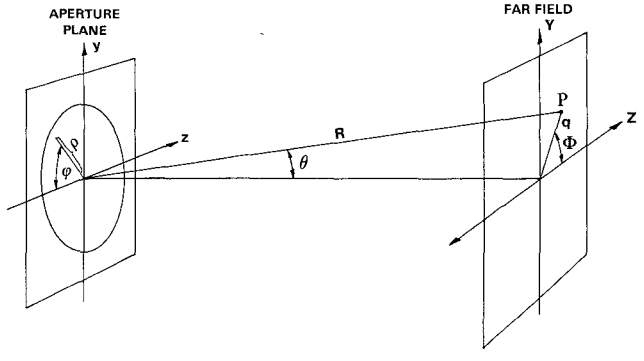

Fig. 10. Geometry for far-field pattern analysis.

After performing the ϕ integration and breaking up the limit on ρ, $E(\theta)$ becomes

$$E(\theta) = \frac{2\pi(1+\cos\theta)e^{j(\omega t - kR)}}{R} e^{-j\delta n} \cdot \left[\int_0^{r_n} F(\rho) J_0(k\rho\sin\theta)\rho\, d\rho - \int_0^{r_{n-1}} F(\rho) J_0(k\rho\sin\theta)\rho\, d\rho\right]$$

so the far-field pattern problem can be reduced to solving the integral

$$I(u) = \int_0^a F(\rho) J_0(u\rho)\rho\, d\rho.$$

Of particular interest in the analysis of Fresnel zone plates is the problem of circular apertures and annuli illuminated by spherical waves. This case has been studied previously by Lommell [10] and Boivin [11], among others. Basically, Fresnel zone plates are designed to convert a spherical wavefront originating at the zone plate focus to an approximately planar wavefront or conversely to convert a planar wavefront to an approximately spherical wavefront converging to the focus [2]. By comparing the derived zone

plate pattern for a spherical wave illumination to the pattern obtained for a plane wave passing through an open aperture with the same dimension as the zone plate, the efficiency of the zone plate wave conversion can be analyzed and special features of zone plate patterns such as spikes in the antenna pattern can be explained analytically.

Using an illumination of $F(\rho) = e^{jk\sqrt{\rho^2+f^2}}$, $I(u)$ can be solved by first changing the variable ρ to $f\sqrt{r^2-1}$. Then the Bessel function is written as a series. The resulting expression is integrated term by term:

$$I(u) = f^2 \sum_{n=0}^{\infty} \frac{(-1)^n}{(n!)^2}\left[\frac{uf}{2}\right]^{2n} \cdot \int_1^{\sqrt{1+(a/f)^2}} e^{jkfr} r(r^2-1)^n \, dr.$$

This integration is carried out by using Euler's formula and the integral for a sine or a cosine multiplied by a polynomial [12]. Let $P_{2n+1}^{(i)}(r)$ be the ith derivative of the $2n+1$ degree polynomial $r(r^2-1)^n$:

$$I(u) = f^2\left(\sum_{n=0}^{\infty} \frac{(-1)^n}{(n!)^2}\left(\frac{uf}{2}\right)^{2n}\left[\frac{\sin kfr}{kf}\sum_{i=0}^{n}(-1)^i \cdot \frac{P_{2n+1}^{(2i)}(r)}{(kf)^{2i}} + \frac{\cos kfr}{kf}\sum_{i=1}^{n}(-1)^{i-1}\frac{P_{2n+1}^{(2i-1)}(r)}{(kf)^{2i-1}}\right] + jf^2\left(\sum_{n=0}^{\infty} \frac{(-1)^n}{(n!)^2}\left(\frac{uf}{2}\right)^{2n}\left[\frac{-\cos kfr}{kf}\sum_{i=0}^{n}(-1)^i \cdot \frac{P_{2n+1}^{(2i)}(r)}{(kf)^{2i}} + \frac{\sin kfr}{kf}\sum_{i=1}^{n}(-1)^{i-1}\frac{P_{2n+1}^{(2i-1)}(r)}{(kf)^{2i-1}}\right]\right)$$

evaluated at the limits of $\sqrt{1+(a/f)^2}$ to 1. If $uf < kf$, the above expression could be simplified by neglecting the higher order derivative terms. As a first-order approximation, only the $i = 0$ terms will be used. This approximation should hold if the $(\frac{uf}{2})^{2n} \cdot \frac{1}{(n!)^2}$ factor converges much faster than the derivative terms increase. For small angles this will be the case.

This form of analysis was applied as a test for the case of a plane wave (uniform phase and amplitude) across a circular aperture of the same size as the zone plate. The resulting plane wave pattern given by the familiar $J_1(x)/x$ (see [8, p. 9-9]). Fig. 11 compares the plane wave pattern with the pattern resulting from the first-order approximation of the derived expressison. The result in Fig. 11 confirms the expected pattern for small angles. An observed characteristic of some measured patterns is the presence of uneven sidelobes and low-level (−30 dB) spikes in the 0–75° range of the pattern. Fig. 9 illustrates a typical zone plate pattern. This particular pattern was measured for a seven-zone, Rexolite/Teflon 35-GHz planar lens. The low-level spikes and uneven sidelobe levels in this pattern are not present in the plane wave or first-order pattern. Analytically these spikes could possibly come from the additional derivative terms which must be included in the expression. These additional terms have an effect similar to adding higher order Bessel functions to the series at larger angles. Edge diffraction would also contribute to these spikes. The far-field or diffraction patterns for Fresnel zone plates and their component annuli have been investigated previously by other authors [11], [13]. Although both of these articles mentioned phase-correcting zone plates, zone plates of alternating opaque and transparent zones were mostly discussed. In addition, these articles considered zone plates with focal lengths large enough ($f \gg \rho$) so that using the binomial series, $\sqrt{\rho^2+f^2}$ can be approximated by $f + \rho^2/2f$ for phase terms and f for amplitude terms [10]. Here ρ is the radial coordinate of the position of the zone plate. The pattern derivation in the present paper requires only that $f > 0$. For many applications a short focal length is desired.

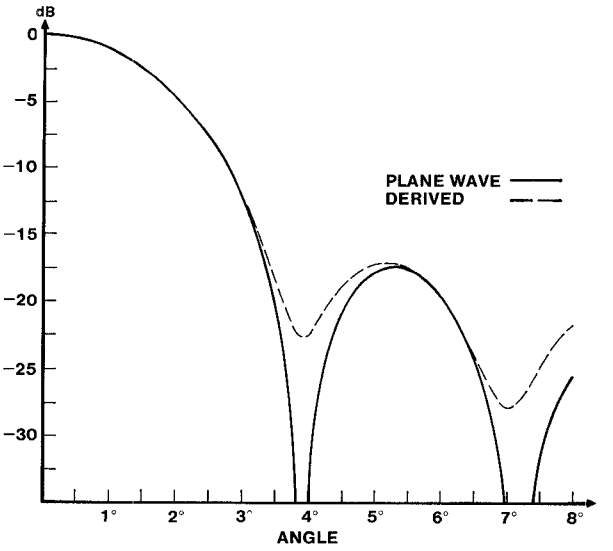

Fig. 11. Plane wave comparison.

VI. Shadowing

Shadowing occurs for the grooved zone plate when radiation originating from one zone of the zone plate must pass through another before reaching a certain point. In this section, an expression for the percentage of zone plate area that is shadowed by other zones will be derived for the case of a normally incident plane wave radiation. The shadowing will occur as the radiation passes through the lens and converges to the focal point. Fig. 12 illustrates the geometry of the shadowing situation. It shows that the radiation passing through the odd zones will be shadowed by the even zones. The area of each zone that is shadowed is given by $\pi(d\tan\theta_n)^2$, where d is the groove depth and $\tan\theta_n$ is given by r_n/f with n an odd integer. The percentage of the total plate that is shadowed is obtained by summing all the individual shadowing zone areas and dividing by the total area of the zone plate:

$$\text{Percentage shadowed} = \frac{\sum_{n=0}^{\text{GIV }[(N-1)/2]} d\pi(\tan\theta_{2n+1})^2}{\text{Area}}.$$

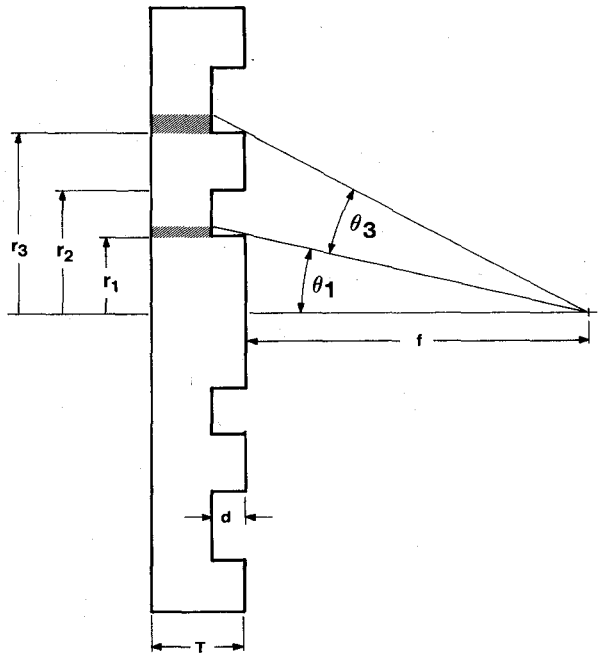

Fig. 12. Shadowing geometry.

The total shadowed area of the zone plate shown in Fig. 2 is 0.05 percent for the plane wave case cited. Obviously, this is a very minor effect in this case.

VII. Conclusion

In this paper the basic design theory and imaging properties of the Fresnel zone plate were presented. A completely flat type of "lens," the planar lens, was discussed. This is a new type of lens that uses the usual zone plate design relations, but it is constructed from two or more different dielectrics of equal thickness.

Zone plates are often used as focusing or frequency-filtering devices. For small angles, the zone plate exhibits a far-field radiation pattern similar to that of a conventional lens, and it exhibits very good off-axis image formation characteristics. The imaging properties illustrate the performance limits of zone plates and can aid in determining when a zone plate can be substituted for a conventional lens. Like a conventional lens, for uniform amplitude illumination zone plates exhibit a 3-dB beamwidth given approximately by $1.029\lambda/2a$ and a first sidelobe level of approximately -17.6 dB, where a is the total zone plate radius. Substituting a zone plate for a lens would be especially desirable if low absorption loss, lower material weight, and flat lens surfaces are important design factors. Zone plates currently find use in applications such as communications and radiometry [5]–[7]. Edge shadowing, an effect found in the zone plate and not in a lens, was discussed in this paper and usually is negligible.

Acknowledgment

The authors would like to acknowledge the assistance of W. A. Seegers, of Martin Marietta Electronic Systems Company, Orlando, FL, who calculated the results in Fig. 7 and measured the antenna pattern in Fig. 9.

References

[1] F. Sobel, F. L. Wentworth, and J. C. Wiltse, "Quasi-optical surface waveguide and other components for the 100- to 300-GHz region," *IRE Trans. Microwave Theory Tech.*, vol. MTT-9, pp. 512–518, Nov. 1961.

[2] J. C. Wiltse, "The Fresnel zone-plate lens," in *Proc. SPIE Symp.* (Arlington, VA), vol. 544, Apr. 9–10, 1985, pp. 41–47.

[3] S. Cornbleet, *Microwave Optics*. New York: Academic Press, 1976, pp. 286–289.

[4] M. Sussman, "Elementary diffraction theory of zone plates," *Amer. J. Phys.*, vol. 28, pp. 394–398, 1960.

[5] J. W. Thornton and J. W. Strozyk, "Multichannel command post radio (MCPR)—An LPI wideband cable replacement radio," in *IEEE Southcon*, Jan. 18–20, 1983, pp. 21/2/1–15.

[6] G. E. Weibel and H. O. Dressel, "Millimeter-wave propagation studies," *Proc. IEEE*, vol. 55, pp. 497–513, Apr. 1967.

[7] M. Cohn, F. Wentworth, F. Sobel, and J. Wiltse, "Radiometer instrumentation for the 1 to 2 millimeter wavelength region," in *Proc. I.R.E. 1962 National Aerospace Electron. Conf.* (Dayton, OH) May 14–16, 1962, pp. 537–541.

[8] J. W. Sherman, "Aperture-antenna analysis," in *Radar Handbook*, M. Skolnik, Ed. New York: McGraw-Hill, 1970, pp. 9-1–9-40.

[9] E. Hecht and A. Zajac, *Optics*. Reading, MA: Addison-Wesley, 1979.

[10] A. Gray and G. B. Matthews, *A Treatise on Bessel Functions and Their Applications to Physics*. London: Macmillan, 1952, pp. 178–221.

[11] A. Boivin, "On the theory of diffraction by concentric arrays of ring-shaped apertures," *J. Opt. Soc. Amer.*, vol. 42, pp. 60–64, Jan. 1952.

[12] J. S. Gradsheteyn and I. M. Ryshik, *Table of Integrals, Series and Products*, New York: Academic Press, 1980.

[13] B. J. Thompson, "Diffraction by semitransparent and phase annuli," *J. Opt. Soc. Amer.*, vol. 55, no. 2, pp. 145–149, Feb. 1965.

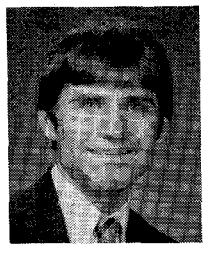

Donald N. Black (S'84) received the B.S.E.E. and M.S.E.E. degrees from the Georgia Institute of Technology in 1986 and 1987, respectively. He is presently working as a graduate research assistant at Georgia Tech and is pursuing the Ph.D. degree. His areas of interest include antenna measurements and their related propagation problems. He is a member of Eta Kappa Nu and Tau Beta Pi.

James C. Wiltse (S'48–A'53–SM'59–F'74) received the B.E.E. and M.E.E. degrees from Rensselaer Polytechnic Institute and the Ph.D. degree from Johns Hopkins University in 1959. His technical interests are in the areas of millimeter- and submillimeter-wave technology, microwaves, lasers, and infrared devices, with applications to communications, radar, radiometry, and guidance.

He has been at Georgia Tech since 1978, initially as a Principal Research Engineer and since 1979 as Associate Director of the Georgia Tech Research Institute. Prior to coming to Tech he spent 14 years with Martin Marietta Corporation, where for four and a half years he was Director of Research and Technology at the Orlando Division. He also served as

Director of Electronics Engineering, Director of Research and Engineering Operations, and Principal Research Scientist. Earlier Dr. Wiltse held a position with Electronic Communications, Inc. for five years, where he was Director of Advanced Technology. He also was employed as a research associate (four years) and an instructor (one year) at Johns Hopkins University, and taught for two years at Rensselaer Polytechnic Institute. He has published about seventy technical articles, four books, and several patent disclosures, and has made numerous presentations at technical meetings and symposia.

Active in the IEEE, Dr. Wiltse is a member of the Editorial Board of the PROCEEDINGS and has been a member of the National Administrative Committee for the Microwave Society (MTT-S), the Editorial Review Boards of the IEEE TRANSACTIONS ON MICROWAVE THEORY AND TECHNIQUES and IEEE TRANSACTIONS ON ANTENNAS AND PROPAGATION, Chairman of the Orlando Section, Chairman and Vice Chairman of the Atlanta Section, and Chairman of Area 3 (Georgia). He was the General Chairman of the 1984 IEEE National Radar Conference, Co-Chairman of the Technical Program for the 1979 International Microwave Conference, and served as the MTT-S National Lecturer during 1979–80 and as a member of the IEEE Delegation to the Soviet Popov Society Meeting in 1979. He recently became a member of the Board of Directors of Southcon, having been the chairman of the Professional Program for Southcon/81 and the Tutorials Committee for Southcon/87. In addition to serving on several technical program committees and as session chairman at various symposia, he has been an Associate Editor of the *Microwave Journal*, General Chairman of three SPIE conferences on millimeter waves, and Co-Chairman, Technical Program Committee, 10th International Conference on Infrared and Millimeter Waves.

Dr. Wiltse is a member of Sigma Xi, Tau Beta Pi, and Eta Kappa Nu, and received the 1975 IEEE Outstanding Engineer of the Year citation for Region 3 (Southeastern U.S.). He is listed in several biographical references.